Climate Change Initiative
Living Planet Fellowship

2014

Robert Parker

University of Leicester

4000112799/14/I-SBo

European Space Agency
Agence spatiale européenne

STANDARD COVER PAGE FOR ESA STUDY CONTRACT REPORTS

<table>
<tr><td colspan="4">ESA STUDY CONTRACT REPORT</td></tr>
<tr><td>ESA Contract No:
4000112799/14/I-SBo</td><td colspan="2">SUBJECT: LPF – ELEGANCE-GHG</td><td>CONTRACTOR: University of Leicester</td></tr>
<tr><td colspan="2">ESA CR( )No:</td><td>No. of Volumes: 1
This is Volume No:1</td><td>CONTRACTOR'S REFERENCE:
RP16G0839</td></tr>
<tr><td colspan="4">ABSTRACT: In this work we examined the spatial-temporal anomalies in atmospheric measurements of CO2 and CH4 and used this information to study some of the underlying processes/assumptions that are utilised by modelling systems to generate and utilise these emissions.

The main results from this work include identification and analysis of enhanced methane emissions from biomass burning of Indonesian peatland driven by the strong El Nino of 2015. The capability to determine not only the enhancement in greenhouse gases from such large fire events but also to identify the dominant combustion processes affecting large regions is valuable as it can provide further constraints on the composition of both the combusting material and the resulting emissions.

This study also performed evaluation of wetland methane emission estimates using satellite CH4 observations. We have shown that a major driver for year-to-year anomalies in tropical methane wetland emissions is seasonal flooding, often related to river overbanking and linked to ENSO variability.</td></tr>
<tr><td colspan="4">The work described in this report was done under ESA Contract. Responsibility for the contents resides in the</td></tr>
<tr><td colspan="4">Names of authors: Robert Parker</td></tr>
<tr><td colspan="2">NAME OF ESA STUDY MANAGER:
Stephen Plummer
DIV: EOP-SC
DIRECTORATE: EOP</td><td colspan="2">ESA BUDGET HEADING:</td></tr>
</table>

CCI Living Planet Fellowship Final Report
ExpLoring thE Global cArboN CyclE through atmospheric GreenHouse Gas variability
Robert Parker – University of Leicester
ELEGANCE

Introduction

One of the major sources of uncertainty in predictions of future global climate is the feedback between climate and terrestrial carbon pools. Friedlingstein et al. (2006) conclude that by the end of the 21st century a larger fraction of anthropogenic CO_2 will remain in the atmosphere due to the changing climate but the magnitude of these effects is widely variable between different models. These estimates ranged from an additional 20 ppm to an addition 200 ppm of CO_2 with the majority of models predicting between 50-100 ppm, leading to an increase in global temperature of between 0.1°C and 1.5°C. It is critical that land system models capture the link between these climatic parameters and the response of carbon pools as this will determine the carbon budget in the future and is hence vital for future climate predictions. In addition to these climatic drivers, major disturbances such as fires and deforestation are also important factors which have to be considered due to their impact upon the carbon exchange to the atmosphere.

CH_4 is the second most important anthropogenic greenhouse gas, with a radiative forcing that is comparable to CO_2 over a 20-year timescale. Methane also influences tropospheric ozone and water vapour, further increasing its importance to the Earth's radiative budget.

In this work I examine the spatial-temporal anomalies in atmospheric measurements of CO2 and CH4 and use this information to study some of the underlying processes/assumptions that are utilised by modelling systems to generate these emissions.

Objectives

The overall objectives of this project were:
1) To identify and quantify the spatial-temporal anomalies in satellite remote sensing data of atmospheric XCO_2 and XCH_4
2) To investigate the key physical climatic drivers for observed atmospheric XCO_2 and XCH_4 anomalies and to assess the representation of these coupling processes in current land system models.
3) To improve our understanding of the role of wetland inter-annual variability on the methane cycle.
4) To quantify the influence that disturbances (such as biomass burning) have on the inter-annual variability of atmospheric CO_2 and the underlying carbon cycle.

In order to achieve these objectives, the project is separated into 4 key tasks, each aligned to one of the objectives

Task 1 – *Identification of XCO_2 and XCH_4 anomalies*
Task 2 – *Analysis of XCO2 anomalies and vegetation response to physical drivers*
Task 3 – *Examining the link between XCH_4 anomalies and the variability of wetland extent*
Task 4 – *Correlation of XCO_2 and XCH_4 anomalies with disturbance events*

After the start of the project, it became obvious that a strong El Nino event was in progress and provided an excellent opportunity to focus on the subsequent extreme biomass burning in more detail than had been originally planned. This result in additional work in Task 4 and hence, less analysis was performed in Task 2.

Task 1 - Identification of XCO_2 and XCH_4 anomalies

This task focused on identifying anomalies in the ESA GHG-CCI data sets. In order to assess the behaviour over time of the greenhouse gas satellite data sets, Hovmoller (latitude-time) plots were produced for each dataset. These were produced by binning all of the quality-flagged data into 1 degree latitude bins for each day. For plotting purposes, a smoothing filter with a length of 5° latitude and 10 days was applied to the datasets. The satellite XCO_2 data was then detrended using the NOAA globally averaged marine surface monthly mean data and a detrended Hovmoller plot was also produced.

Figure 1 shows these Hovmoller plots for the SCIAMACHY BESD data from the University Bremen which covers the full SCIAMACHY lifetime from 2002-2012. Figure 1a shows the original dataset with Figure 1b showing the detrended data. In the original data, we observe both a gradual annual increase in the XCO_2 amount as well as a clear seasonal cycle, peaking in spring/summer and reaching a minimum in the winter months for each hemisphere. The detrended data (Fig. 1b) shows this seasonal cycle and how it differs year to year with an apparent larger draw-down of CO_2 over the tropics and southern hemisphere in 2010/2011 than in previous years.

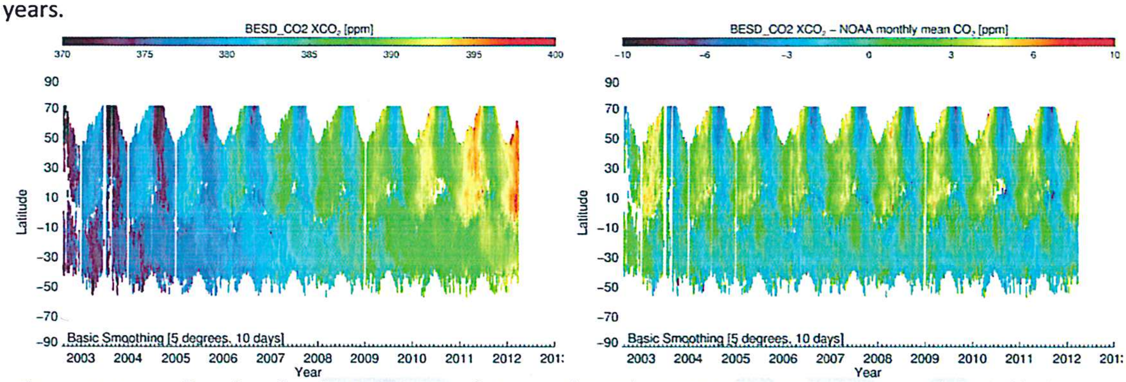

Figure 1: Hovmoller plots for the University of Bremen (BESD) SCIAMACHY XCO_2 timeseries (1a - left) along with a version detrended by the NOAA monthly mean (1b - right)

The same analysis was performed for the GOSAT Full-Physics (OCFP) XCO_2 product from the University of Leicester. Although this dataset covers a shorter time period (2009-2014), it does cover more recent years and is ongoing. Where there is an overlap in time between the GOSAT and SCIAMACHY data, there appears to be a high degree of consistency. The detrended GOSAT data shows even more clearly an enhancement in the CO_2 uptake in 2011 relative to previous year, especially over Australia. This is consistent with findings from Poulter et al., (2014) who conclude that almost 60% of carbon uptake in 2011 is attributed to Australian ecosystems.

In addition to the Hovmoller analysis above, regional timeseries of all of the datasets were analysed. The smoothed timeseries along with the detrended seasonal cycle and growth rates have been calculated using the CCGCRV curve-fitting code (Thoning et al., 1989) rather than relying on auxiliary data to perform the detrending as in Figures 1.

Both the SCIAMACHY AND GOSAT datasets show a largely consistent XCO_2 seasonal cycle and growth rate with several anomalies. In particular both the SCIAMACHY data and the GOSAT data show the decreased growth rate in 2011 which again is consistent with the work above highlighting the strong uptake in 2011 dominated by Australia.

In order to perform a similar analysis for the GOSAT Proxy XCH4 dataset, there is one significant complication that needs to be assessed. As demonstrated by XCH4 from SCIAMACHY (Frankenberg et al., 2006), the Proxy approach exploits the fact that there are CO2 and CH4 spectral signatures located close together at around 1.6um. This leads to similar effects on both species from atmospheric scattering and the ratio of the retrieved XCH_4/XCO_2 should cancel the majority of modifications to the length of the light-path that are experienced due to scattering (Butz et al., 2010). In this way the CO_2 is able to act as a "proxy" for the unknown light-path enhancements. The final product is then obtained by multiplying the XCH_4/XCO_2 ratio by the CO_2 values provided by a global chemistry transport model.

Advantages of the proxy retrieval method are outlined in Schepers et al. (2012) and largely relate to the robustness of the retrieval in the presence of moderate amounts of aerosol, negating the need for accurate a priori knowledge of the aerosol distribution. A consequence of this is that there are typically many more successful soundings for the proxy retrieval than for the full physics approach.

However, the proxy approach does require the use of accurate and unbiased data from an XCO_2 model which itself can add uncertainty into the data product. Here we present assessments of the different uncertainties present in the Proxy XCH_4 data and assess their significance, a vital step before continuing to analyse the data for temporal-spatial anomalies.

For the University of Leicester GOSAT Proxy XCH_4 data an ensemble of XCO_2 models is used to renormalise the XCH_4/XCO_2 ratio. This ensemble comprises three state of the art global transport models which all assimilate surface in-situ measurements; GEOS-Chem (University of Edinburgh v1.50), MACC-II (v14r1) and CarbonTracker (vCT2013B).

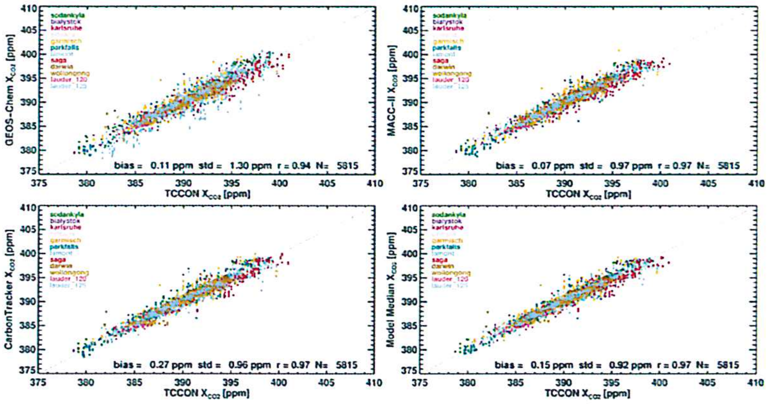

Figure 2: Correlation plot of the model XCO_2 data for GEOS-Chem, MACC-II, CarbonTracker and the ensemble median against TCCON ground-based FTS data at 11 TCCON sites. The overall bias, standard deviation (single-measurement precision), correlation coefficient and total number of soundings are provided separately.

Figure 2 shows the validation of the ensemble median values as well as the individual models making up the ensemble. The model XCO_2 data sampled at each GOSAT measurement point within ±2° of each TCCON station is found to agree well with the TCCON data, with the correlation coefficients ranging from 0.94 (GEOS-Chem) to 0.97 (MACC-II and CarbonTracker). Similarly the precision and bias to TCCON are both found to be small (ranging from 0.97 to 1.3 ppm and 0.07 to 0.27 ppm respectively). By examining the statistics at individual TCCON stations for each of the models it is apparent that it is not possible to identify any one model as being the best, with the ensemble median itself having the best performance against TCCON, hence justifying its use in the Proxy data product.

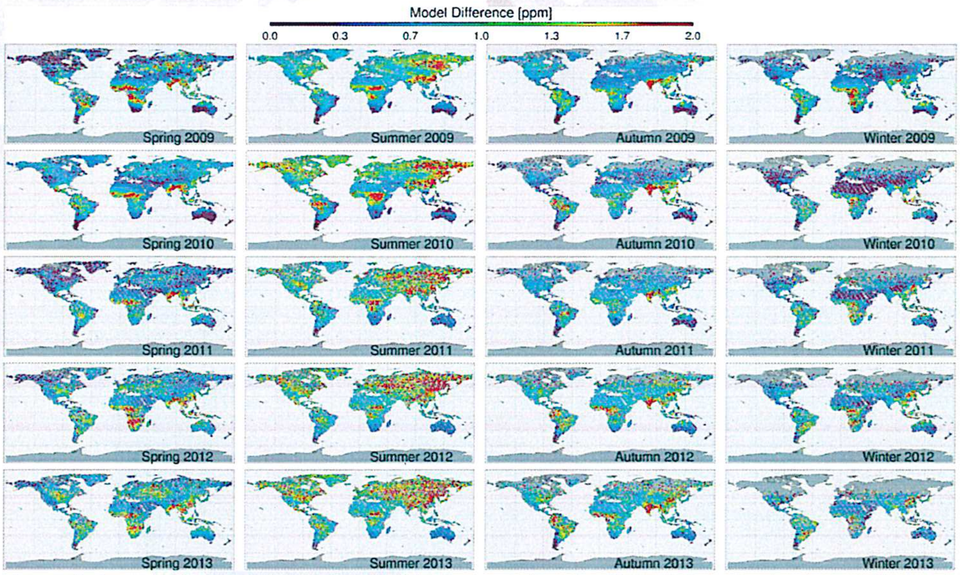

Figure 3: Seasonal maps of the model difference, defined as the maximum absolute difference of the three-model ensemble from the median. All individual soundings have been averaged into 2°x2° grid boxes over each season. The largest uncertainties occur in regions where the CO_2 variability is expected to be highest and the models are unconstrained by surface measurements.

Despite very good agreement at the TCCON locations, it is this uncertainty in model XCO_2 in regions away from the available validation data that has the potential to introduce the largest biases in the data. The use of a model ensemble allows us to make an estimate of this uncertainty by examining the maximum difference of the individual models from the ensemble median. The results from this are shown in Figure 3.

The models are found to disagree with each other by up to 4 ppm in some regions with clear spatial/temporal patterns in the distribution of this model uncertainty. Biomass burning regions such as Africa and India typically show large uncertainties (> 2 ppm) along with the Eurasian/Siberian region during the summer months. This is to be expected as in the Northern Hemisphere it is the period of greatest photosynthetic activity and the model sensitivity to the underlying mechanisms is likely to be largest. A more detailed assessment of this behaviour along with the implications on model flux inversions is provided in Parker et al., 2015.

With the above analyse informing the interpretation of any results it is possible to examine the anomalies in the Proxy XCH4 dataset. In order to do this, we calculate the smoothed detrended seasonal cycle (as performed above for CO2) over the entire dataset. By detrending the dataset, we remove any potential trends relating to the use of the model CO2 in the Proxy method. Calculating the 95th percentile of this dataset allows us to identify regions that have a large anomaly above the global average, thus allowing for "hotspot" detection.

While some work is ongoing in relation to methane hotspot detection in which we are involved (Buchwitz, 2016), the GOSAT sampling pattern makes the instrument non-ideal for such small-scale applications. Nevertheless, we do observe enhanced values over known CH_4 emission regions such as South-East Asia, the Amazon and over the Sudd wetlands in central Africa. The latter is of particular interest as it is at a relatively small scale and not immediately apparent from the original XCH4 satellite data, showing that there is some utility in this technique to identify localised enhancements. While acting as a proof of concept with GOSAT, this technique will potentially be of much more use with the upcoming S5P mission which will provide CH4 measurements at a much higher spatial resolution.

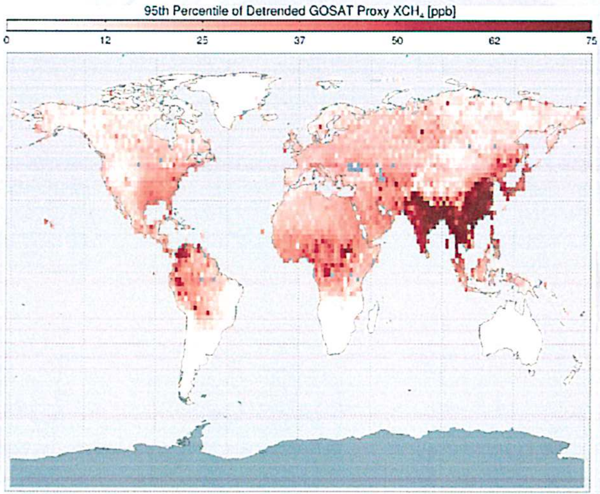

Figure 4: Global map of the 95th percentile of the detrended data over the entire GOSAT Proxy XCH4 timeseries. Regions of known strong methane emissions are apparent over the Amazon, South-East Asia and central Africa.

This work on the Proxy error assessment was successfully published as *Parker, R. J. et al., Assessing 5 years of GOSAT Proxy XCH_4data and associated uncertainties, Atmos. Meas. Tech., 8, 4785-4801, doi:10.5194/amt-8-4785-2015, 2015.*

Task 3 - Examining the link between XCH4 anomalies and the variability of wetland extent

Wetland emission inventories are used to determine the spatial-temporal magnitude of wetland emissions and are widely used as a priori information in model flux inversions. These emissions are either estimated via a top down approach (typically using satellite observations that relate somehow to the wetland extent) or via bottom-up estimation using a land system model. This work will assess inventories created using both methods.

JULES is the Joint UK Land Environment Simulator and forms the land system model component of the UK Earth System Model (UKESM). Methanogenesis, the biogenic production of CH_4, occurs in natural wetlands and rice paddies by the anaerobic degradation of organic matter by methanogenic archaea. Production rates are controlled by the availability of suitable substrates, temperature and soil salinity. This means that emissions can be estimated based on other geophysical parameters produced within JULES, such as soil temperature and wetland fraction (see Equation 1).

$$F_{CH_4} = k_{CH_4} f_w \Lambda Q_{10}(T_{soil})^{(T_{soil}-T_0)/10} \quad \text{(Equation 1)}$$

Wetland CH_4 flux (F_{CH_4}) Calibration constant (k) Wetland fraction (f_w) Total methanogenesis (Λ) Temperature coefficient (Q_{10}) Soil temperature (T_{soil})

In contrast to the bottom-up approach, the top-down approach uses satellite observations. In this work, we use the emission inventories described in Bloom (2010). These are inferred by isolating the wetland and rice paddy contributions to spaceborne CH_4 measurements over 2003-2005 from the SCIAMACHY instrument through the use of satellite observations of gravity anomalies (a proxy for water-table depth) and surface temperature. This data is then used to generate wetland CH_4 emission inventories for 2003-2011. Results from Bloom suggest that tropical emissions are largely described by water-table depth, whilst higher-latitude emissions are more influenced by soil temperature.

In order to more fully assess these emission databases, we compare them to satellite observations. Methane fluxes are not measured directly from satellites, instead we observe total columns of atmospheric methane. In order to compare these observations to the emission data, we make use of a chemistry transport model that takes these wetland emissions (along with our best a priori knowledge of other methane sources) and model the atmospheric concentrations based on these emissions. For this work we have used the TOMCAT atmospheric chemistry transport model ran by colleagues at the University of Leeds (for more details see Chipperfield, 1999) and produced model XCH_4 output using both the JULES and Bloom wetland emission inventories.

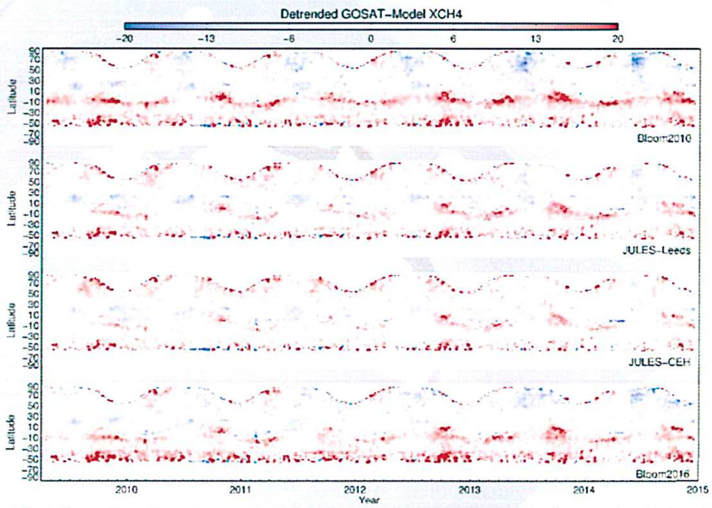

Figure 5: Hovmoller plot showing the detrended GOSAT-Model difference for each of the 4 model simulations.

Figure 5 shows the difference between the detrended GOSAT seasonal cycle and the detrended Model seasonal cycle for each of the 4 model simulations. Generally the difference between observations and model are small (< 5 ppb). The largest differences occur in the tropics, driven by the Amazon region but also contributed to by central Africa and Asia. There is a clear inter-annual variability with some years (such as 2012/2013) showing a greater difference. To explore when and where these differences occur and to understand the processes that lead to them, individual regions are analysed. Figure 6 shows the CIFOR Sustainable Wetlands Adaptation and Mitigation Program (SWAMP). This data has been used to identify the different wetland regions.

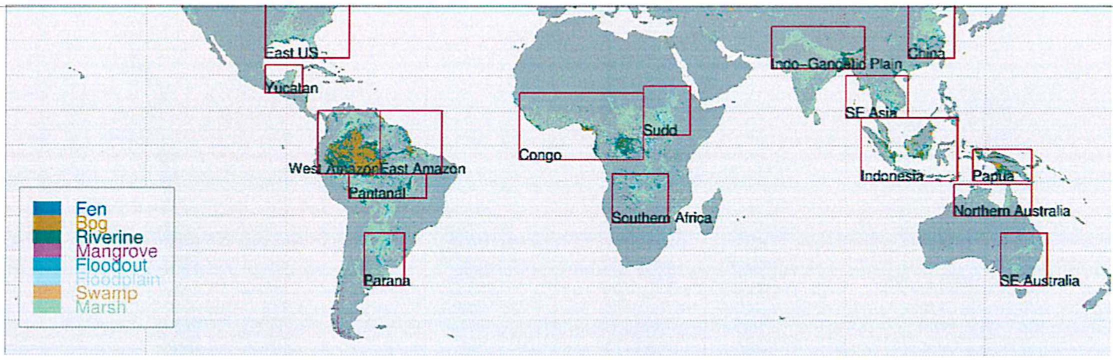

Figure 6: The CIFOR Sustainable Wetlands Adaptation and Mitigation Program (SWAMP) dataset showing the location and type of wetland. This data was used to determine which regions to analyse.

Figure 7 shows the peak to peak seasonal cycle magnitude for each of the wetland regions identified in Figure 6. The seasonal cycle magnitude can range from 10 ppb (e.g. in SE Australia) to almost 100 ppb (e.g. in SE Asia). From this data is it clear that generally all of the models do a reasonable job in capturing the size of the seasonal cycle in most regions in most years. The Asian regions (China, SE Asia, Indonesia and Papua) tend to overestimate the seasonal cycle in the model compared to the observations, likely attributable to the rice emissions used in the model. The other regions are in much closer agreement, although there are certain regions/years where we still observe significant differences. For example, the Pantanal and Parana regions in South America (which include the world's two largest wetland complexes) show significant differences in some years. As a case study, the Parana region is examined in more detail in the following section.

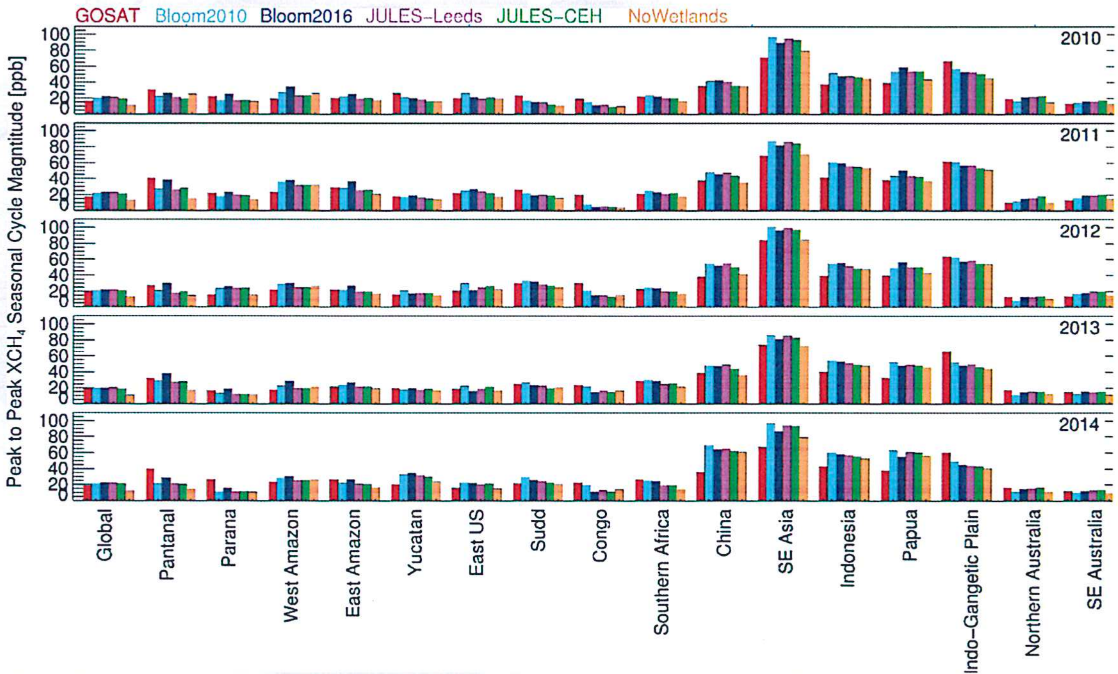

Figure 7: The peak to peak seasonal cycle magnitude for each of the regions of interest for each year.

A significant difference is observed between the GOSAT observations and model differences between November 2009 and February 2010. A map of the detrended GOSAT-JULES difference over the Parana region (Figure 8) for this time period shows a distinct spatial pattern, with JULES having too large emissions to the east of the region and lacking emissions in the centre. From the additional ancillary data, it is clear that JULES is producing emissions in the eastern part of the region where the rainfall occurs but the observations show that the emissions are occurring in the centre of the region, around the Parana River basin. By examining MODIS imagery for this time period (Figure 9) and comparing it to the same period in the subsequent year, we see that there is clearly a significant increase in visible wetland extent related to the river flooding compared to latter years. This river flooding (or overbank inundation), is a process that is not currently reproduced in the JULES model and hence explains why the model does not produce emissions in this area. A simple calculation of the total cumulative methane seasonal cycle signal over this period suggests that the model is only producing approximately 50% of the emissions suggested by observations, making it a significant omission that it is possible to identify through use of the ESA GHG-CCI data and one that should be addressed through further model development.

This work is currently in preparation for submission as a peer-reviewed publication.

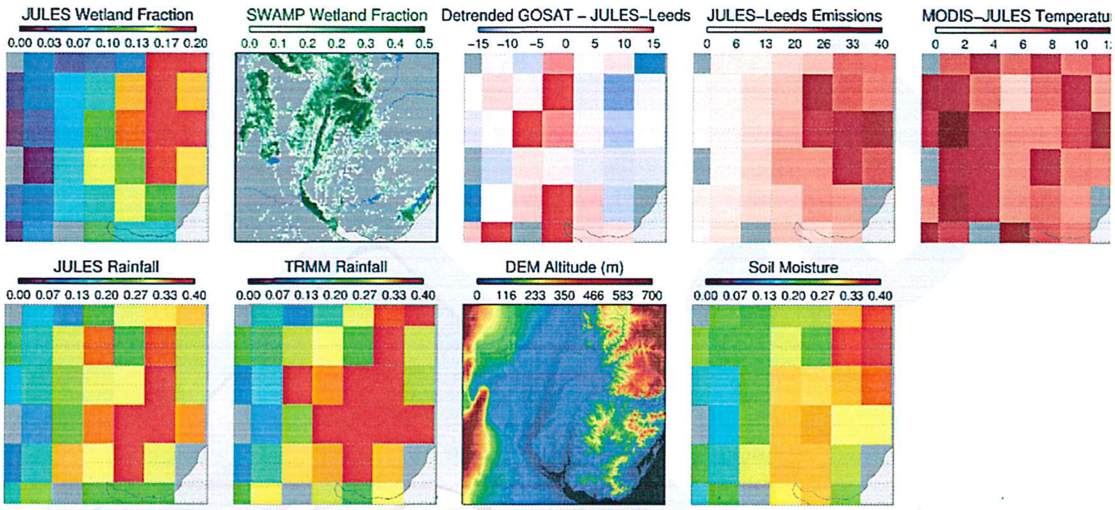

Figure 8: Maps showing the GOSAT-Model difference along with other ancillary data over the Parana region.

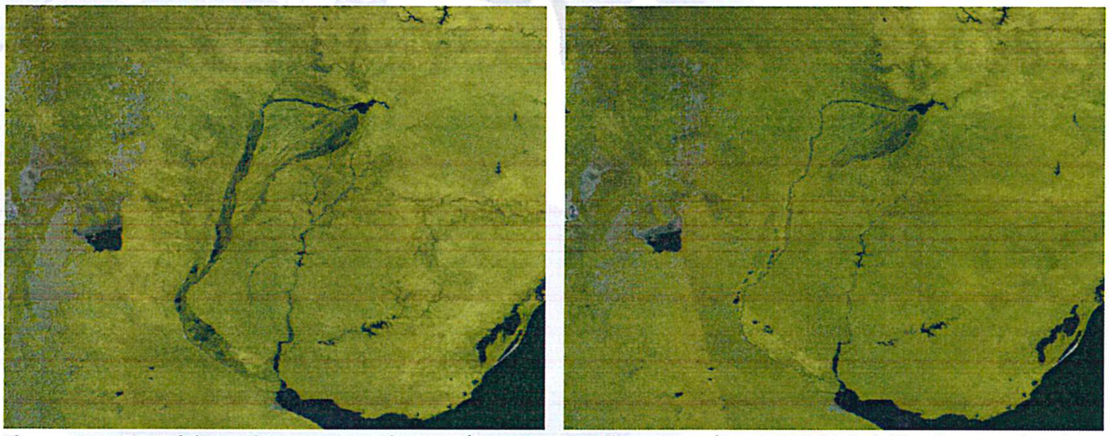

Figure 9: MODIS false-colour imagery for Nov/Dec 2009 (left) and Nov/Dec 2010 (right). The Parana river is clearly shown to have experienced significant flooding in the 2009 period.

Task 4 – Correlation of XCO_2 and XCH_4 anomalies with disturbance events

Wildfire emissions significantly affect various aspects of the Earth system, from local air pollution to global atmospheric chemistry and climate change. Anomalies in both inter-annual variability and the atmospheric growth rate of CO_2 and CH_4 have been attributed to biomass burning events (Kasischke et al., 2002; van der Werf et al. 2004; Simmonds et al., 2005), showing that such wildfire emissions can potentially have a significant effect on climate. The 1997-1998 El Nino event saw estimated carbon emissions from Indonesia of 0.81-2.57 Pg or 13-40% of annual global fossil fuel emissions Page et al. (2002). Even short localised fire events can lead to significant greenhouse gas emissions, as demonstrated by Gaveau et al. (2014) who report that a short (one week) fire event was responsible for emitting 172±59 Tg CO_2-eq, approximately 5-10% of Indonesia's average annual greenhouse gas emissions. These examples highlight the significant nature of such wildfire events and their potential for dramatically affecting the carbon cycle.

When estimating wildfire emissions, emission factors (EF) are used to convert between the amount of fuel burned and the amount of gas emitted (Reid et al, 2005). These EFs are typically determined through the use of emission ratios (ER) which can be obtained through measurement of the ratio of the emitted species (Andreae et al, 2001). We first demonstrated the capability to measure the CH_4/CO_2 ERs from space in Ross et al., (2013) and now extend this work to examining fires over Indonesian driven by the large 2015/2016 El Nino event.

The Indonesian region is particularly strongly affected by El Nino, with the potential for severe drought and warmer temperatures to exacerbate an already delicate ecosystem. Indonesian peatlands are already highly managed, with large areas drained for agricultural use which in turn leads to areas abundant with dry carbon-rich peat that are highly susceptible to wildfires (both natural and anthropogenic, related to land clearance) and capable of releasing significant quantities of greenhouses gases into the atmosphere. During an El Nino event, even peatland areas that are typically too wet to burn under normal circumstances are dried out to such an extent that they also become susceptible to wildfires (Wooster et al., 2012), giving the potential for El Nino to cause even more extreme amounts of fire activity and subsequently larger emissions of greenhouse gases.

In order to investigate the magnitude of the increased fire activity over Indonesia associated with the current El Nino we first examine the fire radiative power (FRP). Fire radiative power is a measure of the thermal radiation identified as being due to actively burning vegetation. This release of thermal radiation is strongly related to fuel consumption and is hence both an indicator for the presence of fire and an estimator for the amount of trace gas emissions from that fire. Global satellite observations of FRP are made from the SEVIRI and MODIS instruments and are incorporated into the Copernicus Monitoring Atmospheric Composition and Climate (MACC) Global Fire Assimilation System (GFAS), providing estimates of trace gas emissions. It should be noted such satellite observations of these fire parameters rely on being able to see the surface and this can prove challenging, in particular when there are large amounts of clouds or fire-related aerosols/smoke. This has the potential to lead to underestimation of the magnitude of the fire.

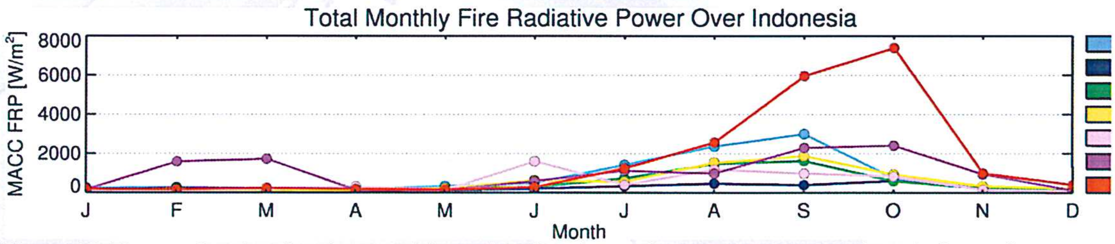

Figure 10: Time series showing the monthly total MACC Fire Radiative Power over Indonesia for each year. Values for September/October 2015 show a significant increase compared to previous years, highlighting the significant effect of El Nino on fire activity in this region. Figure taken from Parker et al, 2016 (in prep).

Figure 10 shows the monthly averaged MACC-GFAS FRP (in W/m^2) over the Indonesian region (defined as 5°N-10S, 90°E-150°E) for 2009-2015. This figure shows that while September/October is the typical burning period for this region, the burning that took place in the latter part of 2015 was an extreme event even in this context, with the total measured FRP for October 2015 exceeding 7500 W/m^2 compared to the second highest value of just over 2000 W/m^2 in October 2014.

The objectives of this work are to first determine whether the expected high concentrations of CH_4 emitted by the extreme peatland burning in September/October 2015 over Indonesia are observable from satellite data and if that is the case, to then determine the emission ratio of CH_4/CO_2 and compare this to measurements made in-situ. The capability to examine the large-scale emission ratios of a region such as this is important because if GOSAT can measure CH_4/CO_2 emission ratios, it is therefore capable of discerning different types of fires and thus can help to discriminate combustion dominated by smouldering processes from that primarily involving flaming processes. Not only is this of direct interest for the CH_4 and CO_2 emissions themselves but is also useful as the chemical composition of smoke can differ greatly between combustion dominated by either flaming or smouldering processes.

In order to quantify the extreme nature of the October 2015 observations and to account for the annual growth rate, we define the magnitude of the enhancement as the October-July difference for each year. For CO_2 we observe a magnitude of 4.35 ppm for October 2015 compared to a mean value of 1.05 ± 1.42 ppm for the previous years (2009-2014). In the case of XCH_4, the enhancement value for October 2015 is found to be 45.65 ppb compared to an average for previous years of 11.93 ± 3.60 ppb. This enhancement of the XCH_4 in October 2015 is therefore significantly higher than that observed over the region in previous years and corresponds to the extreme in fire activity observed in Fig. 10.

The MACC carbon monoxide (CO) data is used to determine if the GOSAT sounding time/location is likely to be affected by fire. After identifying which GOSAT soundings are affected by fire, it then becomes possible to examine the CH_4, CO_2 and XCH_4/XCO_2 distributions for the clear and fire-affected cases to determine the enhancement in emissions due to the fire activity. Figure 11 shows the histograms for the XCH_4/XCO_2 ratio as well as the individual XCH_4 and XCO_2 components for all data (shown in green), for the data identified as unaffected by fire (blue) and finally for the data deemed to be affected by fire (red).

For the XCH_4/XCO_2 ratio, the mean of all data is 4.54 ppb/ppm with a standard deviation of 0.033 ppb/ppm. The distributions for the clear and fire-affected data show two clearly separated distributions with means of 4.52 and 4.59 ppb/ppm respectively. When examining just the CO_2 distributions, there appears to be less of a distinct separation, with means of 399.9 and 401.1 ppm respectively for the clear and fire-affected cases. This corresponds to an increase of just 0.3% percent over the background CO_2 concentrations. In contrast, the CH_4 distribution for the fire-affected scenes is found to be significantly enhanced by 1.9% percent over the background (1840.1 ppb vs 1805.5 ppb).

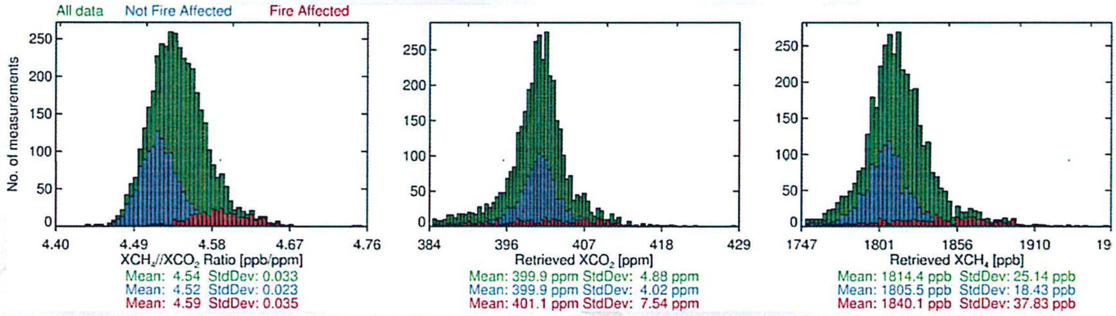

Figure 11: Histograms showing the distributions over Indonesia in September/October 2015 of the XCH_4/XCO_2 Ratio (left), the retrieved XCO_2 (centre) and the retrieved XCH_4 (right) for all data (green), data determined to be unaffected by fire (blue) and data determined to be affected by fire (red). Also included are the corresponding mean and standard deviation values for each distribution. Figure taken from Parker et al, 2016 (in prep).

Having the capability to determine large-scale regional emission ratios during intense fire-activity is important as it allows information to be gained not only on the emissions themselves but also on the characteristics of the fire activity (i.e. flaming vs smouldering combustion). In this work, we use the methodology as in Ross et al. (2013) where we demonstrated for the first time the ability to determine CH_4/CO_2 emission ratios from satellite data. In that work, we derived CH_4/CO_2 emission ratios for boreal forest, tropical forest and savanna fires which were in good agreement with past ground and airborne studies. Here we apply the same technique to the GOSAT measurements during the extreme fire activity over Indonesia in September/October 2015.

In order to calculate the excess (or "Δ"') XCH_4 and XCO_2 values it is necessary to be able to obtain a background concentration from a scene unaffected by fires. In a region such as Indonesia where there is large-scale fire activity affecting much of the area, this aspect becomes much more challenging and requires that care is taken in choosing appropriate and representative background concentrations (Yokelson et al., 2013).

Only fire-affected soundings over land were considered so as to reduce the effect of dilution/mixing due to transport over the ocean. For each fire-affected GOSAT sounding, a background sounding was selected from soundings that were identified as being unaffected by fire according to the MACC CO fields and were located nearby on the same landmass (e.g. the background for the Sumatra soundings were selected from clear soundings between 90°E-108°E and 5°N-10°S). Out of 131 fire-affected soundings, a suitable background sounding was identified for 105 (80%) of the cases. Each background XCH_4 and XCO_2 value was subtracted from its corresponding fire-affected sounding concentration to produce the ΔXCH_4 and ΔXCO_2 values from which the emission ratio can be calculated.

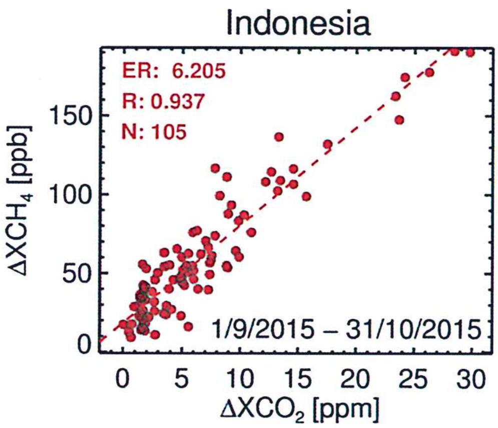

Figure 12: Correlation of the ΔXCH_4 vs ΔXCO_2 values, calculated as the difference between the values in the fire-affected soundings to those in the background cases over the entire Indonesian region for 1st September 2015 to 31st October 2015. The CH_4/CO_2 emission ratio is calculated from the gradient of a linear fit to the data. This line of best fit is also shown, along with the correlation coefficient, R and the number of soundings, N. Figure taken from Parker et al, 2016 (in prep).

Whilst this calculated CH_4/CO_2 emission ratio is significantly above the normal background levels, there is significant variability to the fire activity during this period leading to the potential for many different fire plumes to be sampled and included together in the correlation.

In contrast to the Sumatra region, the Kalimantan region is characterised by typically lower FRP and CO emissions during this period interspersed with short but intensive fire events such as those on 8th September and 14th October. The ER calculated over the whole time period is found to be 6.2 ppb/ppm, calculated from 39 data points with a correlation coefficient of 0.974. When examining the period from 8th-17th September, although derived from only 9 data points with a correlation coefficient of 0.92, the ER is found to be extremely high with a value of 13.6 ppb/ppm. In contrast, the ER for the second time period from 14th-25th October, is found to be similar to that for the overall time period, with an ER of 6.2 ppb/ppm. This is likely due to the fact that throughout this second period, there is extensive smoke/aerosol covering the entire region and as such, any selection of a clear background is significantly more difficult for the most intense phase of the burning. This is further compounded by the fact that the wind vectors for this time period show the actual background air is likely to be coming from further south.

The objective of this study was to utilise GOSAT XCH_4 and XCO_2 observations over Indonesia to identify whether the increase in fire activity related to the ongoing significant El Nino event led to a resulting increase in the XCH_4 atmospheric concentrations. In the event that an increase in CH_4 was observed, the further objective was to apply a similar technique as we demonstrated in Ross et al., (2013) to determine the CH_4/CO_2 emission ratios and confirm that observations over Indonesia are dominated by smouldering combustion in contrast to those in Africa and the Amazon where flaming combustion is expected to result in a lower CH_4/CO_2 ratio.

We find a significant enhancement of XCH_4/XCO_2 in the fire-affected GOSAT soundings, with the majority of this attributed to an enhancement in the XCH_4 mixing ratios where we see an average value of 1840.1 ppb compared to an average value in the clear cases of just 1805.5 ppb. For these fire-affected soundings, the CH_4/CO_2 emission ratio is estimated from the gradient of the linear fit of the excess CH_4 and CO_2 values. We find an overall ER for the entire region of 6.2 ppb/ppm, with Sumatra showing slightly higher values at 6.6 ppb/ppm compared to 6.2 ppb/ppm for Kalimantan. When examining shorter periods of time to focus on specific fire events, we find ERs as high as 13.6 ppb/ppm which is consistent with field-work observations made at the same time.

Furthermore, we were able to show that the emission ratio for the Indonesia region indicates that the emissions are largely dominated by smouldering combustion (e.g. ER > 6) whilst southern Africa has a lower ER (e.g. ER < 4.5) indicating that it is dominated by flaming combustion with the Amazon exhibiting an ER between the two, consistent with prior expectation and previous ground-based studies.

The capability to determine not only the enhancement in greenhouse gases from such large fire events but also to identify the dominant combustion processes affecting large regions is valuable as it can provide further constraints on the composition of both the combusting material and the resulting emissions. There are still some challenges, mainly relating to obtaining an accurate representation of the background value, that prevent this technique from being routinely applied to determining the CH_4/CO_2 emission ratios from the GOSAT satellite.

However, this technique should be easily applicable to future satellite missions with increased spatial/temporal resolution that will aid in obtaining suitable background values. One such mission, Sentinel-5 Precursor, is planned for launch in 2016 and is capable of measuring both CH_4 and CO meaning that it would be ideally suited for application of this technique in determining regional ERs from space.

This work was successfully published as *Parker, R. J. et al., Atmospheric CH_4 and CO_2 enhancements and biomass burning emission ratios derived from satellite observations of the 2015 Indonesian fire plumes, Atmos. Chem. Phys., 16, 10111-10131, doi:10.5194/acp-16-10111-2016, 2016.*

Summary

This project was split into 4 separate work packages with the overall focus on identifying and interpreting anomalies in the GHG datasets. This work was begun in Task 1 with all of the ESA GHG-CCI data analysed. In particular, it was decided that for the Proxy XCH4 data to be confidently utilised, an assessment of any biases introduced by the model CO2 has to be performed. This work was published in Parker et al., (2015).

As a strong El Nino event was identified as being in progress at the start of this project, the focus was shifted more heavily onto Task 4 which dealt with analysing anomalies related to disturbance events such as fires. From this work we were able to successfully attribute observed enhancements in CO2 and CH4 in the Indonesian region to the significant increase in fire activity and furthermore, were able to successfully determine the CH4/CO2 emission ratio of these fires from the satellite data. The capability to be able to determine such an emission ratio for a large-scale fire event is vital to accurately modelling the atmospheric emissions, which in turn is important for both climate and air quality applications. This work was published in Parker et al., (2016).

Finally, the inter-annual variability of wetland methane emissions has been studied through the use of the ESA GHG-CCI CH4 data, allowing assessment of the different methane emission databases. Overall, good agreement was found between the observations and models, whether the emissions were from top-down or bottom-up databases. A detailed analysis of the methane emission data generated by the JULES land system model showed that the model significantly underestimated (by 50%) the emissions in the Parana region of South America. This was attributed to the lack of capability to model wetland extent generated through overbank inundation during large flooding events. This work is currently being written up for publication.

Overall, I consider that the project was successful, leading to 3 first author publications, along with 14 co-authored publications. I have also performed significant analysis of the GHG-CCI datasets, working closely with the data providers to interpret and improve the satellite data. Future work beyond the end of this project will continue to focus on the assessment and evaluation of data generated by the UK Earth System Model, of which the ESA CCI data will continue to provide vital evaluation capabilities.

Publications (since project start – March 2015)

First author:

Parker, R. J. et al., Assessing 5 years of GOSAT Proxy XCH_4data and associated uncertainties, Atmos. Meas. Tech., 8, 4785-4801, doi:10.5194/amt-8-4785-2015, 2015.

Parker, R. J. et al., Atmospheric CH_4 and CO_2 enhancements and biomass burning emission ratios derived from satellite observations of the 2015 Indonesian fire plumes, Atmos. Chem. Phys., 16, 10111-10131, doi:10.5194/acp-16-10111-2016, 2016.

Co-authored:

Buchwitz, M. et al., The Greenhouse Gas Climate Change Initiative (GHG-CCI): Comparison and quality assessment of near-surface-sensitive satellite-derived CO2 and CH4 global data sets, Remote Sensing of Environment, Volume 162, 1 June 2015, Pages 344-362, ISSN 0034-4257, doi:10.1016/j.rse.2013.04.024

Turner, A. J. et al., Estimating global and North American methane emissions with high spatial resolution using GOSAT satellite data, Atmos. Chem. Phys., 15, 7049-7069, doi:10.5194/acp-15-7049-2015, 2015.

Worden, J. R. et al., Quantifying lower tropospheric methane concentrations using GOSAT near-IR and TES thermal IR measurements, Atmos. Meas. Tech., 8, 3433-3445, doi:10.5194/amt-8-3433-2015, 2015.

Berchet, A. et al., Natural and anthropogenic methane fluxes in Eurasia: a mesoscale quantification by generalized atmospheric inversion, Biogeosciences, 12, 5393-5414, doi:10.5194/bg-12-5393-2015, 2015.

Lindqvist, H. et al., Does GOSAT capture the true seasonal cycle of carbon dioxide?, Atmos. Chem. Phys., 15, 13023-13040, doi:10.5194/acp-15-13023-2015, 2015.

Alexe, M. et al., Inverse modelling of CH_4 emissions for 2010–2011 using different satellite retrieval products from GOSAT and SCIAMACHY, Atmos. Chem. Phys., 15, 113-133, doi:10.5194/acp-15-113-2015, 2015.

Feng, L. et al., Estimates of European uptake of CO_2 inferred from GOSAT X_{CO2} retrievals: sensitivity to measurement bias inside and outside Europe, Atmos. Chem. Phys., 16, 1289-1302, doi:10.5194/acp-16-1289-2016, 2016.

Belikov, D. A. et al., Study of the footprints of short-term variation in XCO_2 observed by TCCON sites using NIES and FLEXPART atmospheric transport models, Atmos. Chem. Phys., 17, 143-157, doi:10.5194/acp-17-143-2017, 2017.

Buchwitz, M. et al., Satellite-derived methane hotspot emission estimates using a fast data-driven method, Atmos. Chem. Phys. Discuss., doi:10.5194/acp-2016-755, in review, 2016.

Webb, A. J., et al., CH_4 concentrations over the Amazon from GOSAT consistent with in situ vertical profile data, J. Geophys. Res. Atmos., 121, 11,006–11,020, 2016, doi:10.1002/2016JD025263.

Siddans, R. et al., Global height-resolved methane retrievals from the Infrared Atmospheric Sounding Interferometer (IASI) on MetOp, Atmos. Meas. Tech. Discuss., doi:10.5194/amt-2016-290, in review, 2016.

Feng, L. et al., Consistent regional fluxes of CH_4 and CO_2 inferred from GOSAT proxy XCH_4:XCO_2 retrievals, 2010–2014, Atmos. Chem. Phys. Discuss., doi:10.5194/acp-2016-868, in review, 2016.

McNorton, J. et al., Role of regional wetland emissions in atmospheric methane variability, Geophys. Res. Lett., 43, 11,433–11,444, 2016, doi:10.1002/2016GL070649.

Buchwitz, M. et al., Global satellite observations of column-averaged carbon dioxide and methane: The GHG-CCI XCO2 and XCH4 CRDP3 data set, Remote Sensing of Environment, Available online 9 January 2017, ISSN 0034-4257, doi:10.1016/j.rse.2016.12.027.

References

Alexe, M., Bergamaschi, P., Segers, A., Detmers, R., Butz, A., Hasekamp, O., Guerlet, S., Parker, R., Boesch, H., Frankenberg, C., Scheepmaker, R., Dlugokencky, E., Sweeney, C., Wofsy, S., and Kort, E.: Inverse modelling of CH4 emissions for 2010-2011 using different satellite retrieval products from GOSAT and SCIAMACHY, Atmospheric Chemistry and Physics, 15, 113–133, doi:10.5194/acpd-14- 5 11493-2014, 2015.

Andreae, M. O. and Merlet, P.: Emission of trace gases and aerosols from biomass burning, Global biogeochemical cycles, 15, 955–966, 2001.

Bloom A.A., Palmer P.I., Fraser A., Reay D.S., Frankenberg C. Large-scale controls of methanogenesis inferred from methane and gravity spaceborne data. Science 327:322–325, 2010

Bloom, A. A., Bowman, K., Lee, M., Turner, A. J., Schroeder, R., Worden, J. R., Weidner, R., McDonald, K. C., and Jacob, D. J.: A global wetland methane emissions and uncertainty dataset for atmospheric chemical transport models, Geosci. Model Dev. Discuss., doi:10.5194/gmd-2016-224, in review, 2016.

Buchwitz, M., Schneising, O., Reuter, M., Heymann, J., Krautwurst, S., Bovensmann, H., Burrows, J. P., Boesch, H., Parker, R. J., Detmers, R. G., Hasekamp, O. P., Aben, I., Butz, A., and Frankenberg, C.: Satellite-derived methane hotspot emission estimates using a fast data-driven method, Atmos. Chem. Phys. Discuss., doi:10.5194/acp-2016-755, in review, 2016.

Chipperfield, M. P.: Multiannual simulations with a three dimensional chemical transport model, J. Geophys. Res.-Atmos., 104, 1781–1805, doi:10.1029/98JD02597, 1999.

Cox, P. et al., 2013, Sensitivity of tropical carbon to climate change constrained by carbon dioxide variability, Nature, 494, 341–344, doi:10.1038/nature11882

Cressot, C., Chevallier, F., Bousquet, P., Crevoisier, C., Dlugokencky, E. J., Fortems-Cheiney, A., Frankenberg, C., Parker, R., Pison, I., Scheepmaker, R. A., Montzka, S. A., Krummel, P. B., Steele, L. P., and Langenfelds, R. L.: On the consistency between global and 15 regional methane emissions inferred from SCIAMACHY, TANSO-FTS, IASI and surface measurements, Atmospheric Chemistry and Physics, 14, 577–592, doi:10.5194/acp-14-577-2014, 2014.

Dlugokencky, E. J., et al. 2009, Observational constraints on recent increases in the atmospheric CH4 burden, Geophys. Res. Lett., 36, L18803, doi:10.1029/2009GL039780

Dlugokencky, E., NOAA/ESRL (www.esrl.noaa.gov/gmd/ccgg/trends_ch4/), accessed 1st October 2016.

Frankenberg, C., Meirink, J. F., Bergamaschi, P., Goede, A. P. H., Heimann, M., Körner, S., Platt, U., van Weele, M., and Wagner, T.: Satellite chartography of atmospheric methane from SCIAMACHY on board ENVISAT: Analysis of the years 2003 and 2004, Journal of Geophysical Research: Atmospheres, 111, n/a–n/a, doi:10.1029/2005JD006235, d07303, 2006.

Fraser, A., Palmer, P. I., Feng, L., Boesch, H., Cogan, A., Parker, R., Dlugokencky, E. J., Fraser, P. J., Krummel, P. B., Langenfelds, R. L., O'Doherty, S., Prinn, R. G., Steele, L. P., van der Schoot, M., and Weiss, R. F.: Estimating regional methane surface fluxes: the relative importance of surface and GOSAT mole fraction measurements, Atmospheric Chemistry and Physics, 13, 5697–5713, doi:10.5194/acp-13-5697-2013, 2013.

Fraser, A., Palmer, P. I., Feng, L., Bösch, H., Parker, R., Dlugokencky, E. J., Krummel, P. B., and Langenfelds, R. L.: Estimating regional fluxes of CO2 and CH4 using space-borne observations of XCH4: XCO2, Atmospheric Chemistry and Physics, 14, 12 883–12 895, doi:10.5194/acp-14-12883-2014, 2014.

Friedlingstein, P. et al.,2006, Climate-carbon cycle feedback analysis, results from the C4MIP model intercomparison, J. Climate, 19, 3337-3353, doi:10.1175/JCLI3800.1

Gatti, L., et al., 2014, Drought sensitivity of Amazonian carbon balance revealed by atmospheric measurements, Nature, 506, 76–80, doi:10.1038/nature12957

Gaveau, D. L., Salim, M. A., Hergoualc'h, K., Locatelli, B., Sloan, S., Wooster, M., Marlier, M. E., Molidena, E., Yaen, H., DeFries, R., et al.: Major atmospheric emissions from peat fires in Southeast Asia during non-drought years: evidence from the 2013 Sumatran fires, Scientific reports, 4, 2014.

Gedney, N., P. M. Cox, *and* C. Huntingford *(*2004*),* Climate feedback from wetland methane emissions*,* Geophys. Res. Lett.*,* 31*, L20503, doi:*10.1029/2004GL020919.

Giglio, L., Descloitres, J., Justice, C. O., and Kaufman, Y. J.: An enhanced contextual fire detection algorithm for MODIS, Remote sensing of environment, 87, 273–282, 2003.

Guerlet, S., et al., 2013, Reduced carbon uptake during the 2010 Northern Hemisphere summer from GOSAT, Geophysical Research Letters, Vol. 40, Issue 10, pp. 2378-2383, doi:10.1002/grl.50402

Huntingford, C., et al., 2013, Simulated resilience of tropical rainforests to CO2-induced climate change, Nature Geoscience, 6, 268–273, doi:10.1038/ngeo1741

Kasischke, E. S. and Bruhwiler, L. P.: Emissions of carbon dioxide, carbon monoxide, and methane from boreal forest fires in 1998, Journal of Geophysical Research: Atmospheres, 107, FFR 2–1–FFR 2–14, doi:10.1029/2001JD000461, 8146, 2002.

Keppel-Aleks, G., et al., 2011, Sources of variations in total column carbon dioxide, Atmos. Chem. Phys., 11, 3581-3593, doi:10.5194/acp-11-3581-2011

Kuze, A., Suto, H., Nakajima, M., and Hamazaki, T.: Thermal and near infrared sensor for carbon observation Fourier-transform spectrometer on the Greenhouse Gases Observing Satellite for greenhouse gases monitoring, Applied Optics, 48, 6716–6733, doi:10.1364/AO.48.006716, 2009.

Kuze, A., suto, H., Shiomi, K., Kawakami, S., Tanaka, M., Ueda, Y., Deguchi, A., Yoshida, J., Yamamoto, Y., Kataoka, F., Taylor, T. E., and Buijs, H.: Update on GOSAT TANSO-FTS performance, operations, and data products after more than six years in space, Atmospheric Measurement Techniques Discussions, 2016, 1–38, doi:10.5194/amt-2015-333, 2016.

Melton, J. R., et al., 2013, Present state of global wetland extent and wetland methane modelling: conclusions from a model inter-comparison project (WETCHIMP), Biogeosciences, 10, 753-788, doi:10.5194/bg-10-753-2013

O'Dell, C.W., Connor, B., Bösch, H., O'Brien, D., Frankenberg, C., Castano, R., Christi, M., Eldering, D., Fisher, B., Gunson, M., McDuffie, J., Miller, C. E., Natraj, V., Oyafuso, F., Polonsky, I., Smyth, M., Taylor, T., Toon, G. C., Wennberg, P. O., and Wunch, D.: The ACOS CO2 retrieval algorithm - Part 1: Description and validation against synthetic observations, Atmospheric Measurement Techniques, 5, 99–121, doi:10.5194/amt-5-99-2012, 2012.

Page, S. E., Siegert, F., Rieley, J. O., Boehm, H.-D. V., Jaya, A., and Limin, S.: The amount of carbon released from peat and forest fires in Indonesia during 1997, Nature, 420, 61–65, 2002.

Parker, R., Boesch, H., Cogan, A., Fraser, A., Feng, L., Palmer, P. I., Messerschmidt, J., Deutscher, N., Griffith, D. W., Notholt, J., et al.: Methane observations from the Greenhouse Gases Observing SATellite: Comparison to ground-based TCCON data and model calculations, Geophysical Research Letters, 38, 2011.

Parker, R. J., Boesch, H., Byckling, K., Webb, A. J., Palmer, P. I., Feng, L., Bergamaschi, P., Chevallier, F., Notholt, J., Deutscher, N., Warneke, T., Hase, F., Sussmann, R., Kawakami, S., Kivi, R., Griffith, D. W. T., and Velazco, V.: Assessing 5 years of GOSAT Proxy XCH4 data and associated uncertainties, Atmospheric Measurement Techniques, 8, 4785–4801, doi:10.5194/amt-8-4785-2015, 2015.

Poulter, B, D Frank, P Ciais, RB Myneni, N Andela, J Bi, G Broquet, JG Canadell, F Chevallier, YY Liu, SW Running, S Sitch and GR van der Werf. 2014. Contribution of semi-arid ecosystems to interannual variability of the global carbon cycle., Nature, 509, 600–603 (29 May 2014), doi:10.1038/nature13376

Rigby, M., et al. 2008, Renewed growth of atmospheric methane, Geophys. Res. Lett., 35, L22805, doi:10.1029/2008GL036037

Ross, A. N., Wooster, M. J., Boesch, H., and Parker, R.: First satellite measurements of carbon dioxide and methane emission ratios in wildfire plumes, Geophysical Research Letters, 40, 4098–4102, doi:10.1002/grl.50733, 2013.

Schepers, D., Guerlet, S., Butz, A., Landgraf, J., Frankenberg, C., Hasekamp, O., Blavier, J.-F., Deutscher, N. M., Griffith, D.W. T., Hase, F., Kyro, E., Morino, I., Sherlock, V., Sussmann, R., and Aben, I.: Methane retrievals from Greenhouse Gases Observing Satellite (GOSAT) shortwave infrared measurements: Performance comparison of proxy and physics retrieval algorithms, Journal of Geophysical Research: Atmospheres (1984–2012), 117, doi:10.1029/2012JD017549, 2012.

Simmonds, P., Manning, A., Derwent, R., Ciais, P., Ramonet, M., Kazan, V., and Ryall, D.: A burning question. Can recent growth rate anomalies in the greenhouse gases be attributed to large-scale biomass burning events?, Atmospheric Environment, 39, 2513 – 2517, doi:http://dx.doi.org/10.1016/j.atmosenv.2005.02.018, 2005.

Turner, A., Jacob, D.,Wecht, K., Sulprizio, M., Payne, V., Santoni, G.,Wofsy, S., Bowman, K., Parker, R., and Boesch, H.: Optimal estimation of North American methane emissions using GOSAT data: A contribution to the NASA Carbon Monitoring System, in: AGU Fall Meeting Abstracts, vol. 1, p. 08, 2013.

van der Werf, G. R., Randerson, J. T., Collatz, G. J., Giglio, L., Kasibhatla, P. S., Arellano, A. F., Olsen, S. C., and Kasischke, E. S.: Continental-Scale Partitioning of Fire Emissions During the 1997 to 2001 El Niño/La Niña Period, Science, 303, 73–76, 2004.

Wecht, K., Jacob, D., Sulprizio, M., Santoni, G., Wofsy, S., Parker, R., Bösch, H., and Worden, J.: Spatially resolving methane emissions in California: constraints from the CalNex aircraft campaign and from present (GOSAT, TES) and future (TROPOMI, geostationary) satellite observations, Atmospheric Chemistry and Physics Discussions, 14, 4119–4148, doi:10.5194/acp-14-8173-2014, 2014.

Wooster, M., Perry, G., and Zoumas, A.: Fire, drought and El Niño relationships on Borneo (Southeast Asia) in the pre-MODIS era (1980–2000), Biogeosciences, 9, 317–340, 2012.

Yokelson, R. J., Andreae, M. O., and Akagi, S.: Pitfalls with the use of enhancement ratios or normalized excess mixing ratios measured in plumes to characterize pollution sources and aging, Atmospheric Measurement Techniques, 6, 2155, 2013.